JOURNAL OF MATERIALS SCIENCE 31 (1996) 5463–5469

Microstructure and mechanical properties of silicon carbide fibre-reinforced aluminium nitride composite

K. PARK
Department of Materials Engineering, Chung-ju National University, Chungju, South Korea
T. VASILOS
Department of Chemical and Nuclear Engineering, University of Massachusetts, Lowell, MA 01854, USA

SiC continuous fibre (15 vol %)/AlN composite was fabricated using a sintering additive of $4Ca(OH)_2 \cdot Al_2O_3$ by hot-pressing at 1650 °C and 17.6 MPa in vacuum. Analytical transmission electron microscopy and scanning electron microscopy were used to investigate the microstructure of as-fabricated and crept SiC fibre/AlN composites. The room-temperature mechanical and high-temperature creep properties of the composite were investigated by four-point bending. The incorporation of SiC fibre into AlN matrix improved significantly the room-temperature mechanical properties. This improvement could result from the crack deflections around the SiC fibres. However, the incorporation degraded severely the high-temperature creep properties under oxidizing atmosphere. This could be attributed to the development of the pores and various oxides at the matrix grain boundary and matrix/fibre interface during creep test.

1. Introduction

Aluminium nitride (AlN) is a promising candidate for high-temperature structural applications because of its high melting point, high temperature strength, stiffness, oxidation resistance, and low density. In addition, AlN has recently received much attention as an electronic substrate material because of its high thermal conductivity, high electrical resistivity, and thermal expansion coefficient close to that of Si [1]. However, AlN is extremely brittle so that it fails in a brittle fashion with very little deformation to failure. This can be a major problem when it is utilized in weight-bearing areas of structural applications. Fibre reinforcement may be one of the promising strategies to strengthen AlN. In the present study, an attempt was made to improve the fracture toughness of AlN by the incorporation of SiC (SCS-6^{TM}) fibre in a unidirectional array. The SiC fibre is one of the most important reinforcements for ceramic– and metal–matrix composites due to its high tensile strength (3450 MPa), high tensile modulus (400 GPa), and low density (3.0 g cm^{-3}) [2].

Generally, the densification of pure AlN is difficult because of its covalent bonding, especially at a sintering temperature below 1800 °C. Therefore, several sintering additives, such as CaO [1], Y_2O_3 [3], and MgO [4], have previously been used to fabricate fully dense AlN. In this work, $4Ca(OH)_2 \cdot Al_2O_3$ sintering additive was used to fabricate the SiC continuous fibre/AlN composite by hot-pressing in vacuum.

2. Experimental procedures

Commercial grade AlN powder, SiC (SCS-6^{TM}) fibre, and $4Ca(OH)_2 \cdot Al_2O_3$ sintering additive were used in this study. The sintering additive was used so that a densification temperature could be low in order to minimize the fibre degradation. The properties of the AlN powder used are summarized in Table I. The AlN powders combined with 6 wt % $4Ca(OH)_2 \cdot Al_2O_3$ were mixed with methanol to form a slurry. The resulting slurry was milled using Si_3N_4 balls and then dried in a drying oven. The SiC fibres were wound onto plastic foils unidirectionally with a linear density of 2 fibres/mm and then fixed using a sprayed Krylon type adhesive in order to avoid contact between the fibres. The fibre foils were dried and then cut into small sections (54 × 54 mm). The dried mixtures of AlN and $4Ca(OH)_2 \cdot Al_2O_3$ were poured into the fibre foils in the press die cavity (54 × 54 mm). The die cavity and punch were coated by a thin layer of boron nitride (BN) in order to avoid reaction with a graphite die. The applied pressure was 5.9 MPa when the furnace temperature reached 1200 °C. The applied pressure increased up to 17.6 MPa at 1600 °C. It was maintained at 17.6 MPa and 1650 °C for 2 h and then cooled. The fabricated composite was machined into rectangular bars (3 × 4 × 45 mm), in which the fibres are parallel to the long axis.

The surface morphology of as-fabricated and crept SiC fibre/AlN composites was examined by scanning electron microscopy (SEM) using an Amray 1400 scanning electron microscope. More detailed

0022–2461

TABLE I Properties of AlN powder

Chemical composition	
Al	66.0 wt %
N	32.0 wt %
C	0.1 wt %
O	1.3 wt %
Si	< 168 p.p.m.
Fe	< 112 p.p.m.
Ca	< 25 p.p.m.
Particle diameter	1.8 μm
Specific surface area	2.5 $m^2 g^{-1}$

microstructural information on the composites was obtained from transmission electron microscopy (TEM). Cross-sectional TEM specimens were sectioned from the composite with a low-speed diamond saw. The specimens were mechanically ground to ~ 300 μm. The circular discs of 3 mm diameter were core-drilled from the ground sections. The specimens were mechanically ground to ~ 120 μm and dimpled to ~ 30 μm. The specimens were then ion-milled with 5 kV Ar^+ ions at an incident angle of 12° until perforation was achieved. A light carbon film was evaporated on the specimens in order to prevent charging in the electron microscope. The microstructure of the composite was investigated by a bright field image, selected area diffraction (SAD), convergent beam electron diffraction (CBED), and energy dispersive X-ray spectroscopy (EDXS) using a Philips EM400T TEM and a Noran ultrathin window Micro-Z detector. The mechanical properties of the composite were measured at room temperature and a crosshead speed of 0.5 mm min^{-1} by four-point bending in accordance with ASTM D790 [5] and ASTM C1161 [6] standards using an Instron universal testing machine. The high-temperature creep behaviours of the composite were investigated by four-point bending at 1100 °C and a bending stress of 46.3 MPa for 48 h under oxidizing atmosphere.

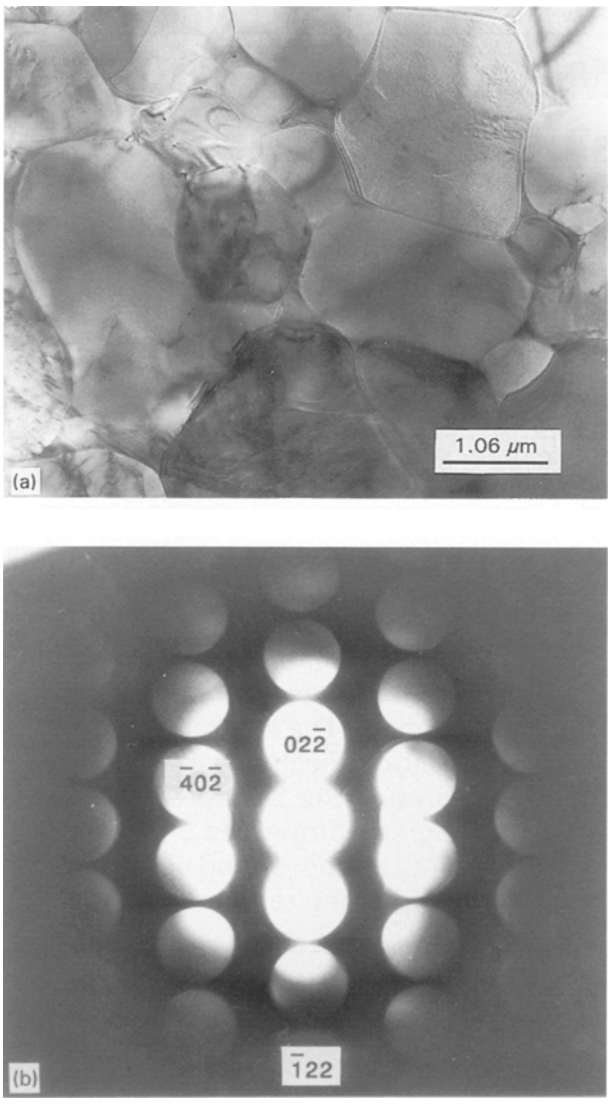

Figure 1 (a) Bright field image of the AlN matrix in as-fabricated composite. The matrix contained a $Ca_{12}Al_{14}O_{33}$ liquid phase at the grain boundaries and dislocations within grains. (b) CBED pattern obtained from the liquid phase at the grain boundaries.

3. Results and discussion

3.1. Microstructure of as-fabricated SiC fibre/AlN composite

Generally, the microstructure of AlN matrix in as-fabricated composite was very dense (up to ~ 99% of theoretical density) and fine grained. As shown in Fig. 1(a), the matrix contained rounded grains and dislocations within grains. The $Ca_{12}Al_{14}O_{33}$ liquid phase with a cubic structure (a = 1.198 nm) was present at grain boundaries. A CBED pattern obtained from the liquid phase is shown in Fig. 1(b). This result indicates that some of the $4Ca(OH)_2 \cdot Al_2O_3$ sintering additive was present in the liquid phase at the grain boundaries. The volume fraction of the liquid phase was estimated as ~3.0 %.

The SiC fibre in as-fabricated composite was uniformly distributed through the matrix. In particular, the fibre was not degraded during fabrication because of relatively low sintering temperature (1650 °C), thus showed clearly several different layers (core carbon, inner carbon layer, SiC layer, and outer carbon layer), like the unprocessed SiC (SCS-6™) fibre. Since Al in the matrix diffused into the fibre during fabrication, the SiC layer contained a small amount of Al (Fig. 2(a)) to form SiC–Al solid solutions with a cubic structure (a = 0.435 nm) (Fig. 2(b)). The solubility of Al in SiC at 2200 °C has been reported as 1.0 wt % [7]. Small equiaxed SiC grains were often observed on the outside of the columnar SiC grains before the growing of the outer carbon layer, as shown in Fig. 3. SiC particles in the outer carbon layer are indicated by arrowheads.

Fig. 4(a) shows that the AlN matrix reacted with the outermost carbon layer in the fibre during fabrication. Unreacted sublayers in the outer carbon layer are indicated by A, B, and C, and the reacted layer of the outermost carbon layer and AlN matrix is indicated by D. In the unreacted sublayers, SiC particles were embedded in the turbostratic carbon. The SAD pattern obtained from the unreacted sublayers was composed of distinctive arcs and randomly distributed spots, indicating a preferred alignment of turbostratic carbon blocks and an existence of SiC particles. The reacted layer D was mainly composed of

C–Al–Ca–O (bright area) and Si–Al–C–O (dark area) phases.

Fig. 4(b) and (c) show a CBED pattern and EDXS spectrum obtained from the C–Al–Ca–O phase in the reacted layer D, respectively. The C–Al–Ca–O phase was formed by the reaction of carbon in the outermost carbon layer and Al, Ca, and O in the matrix during fabrication. Although the bright areas contain a small amount of Al, Ca, and O along with carbon, they have a preferentially oriented carbon structure, which is

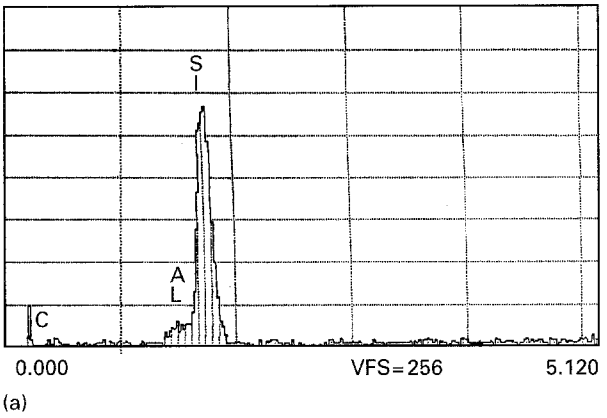

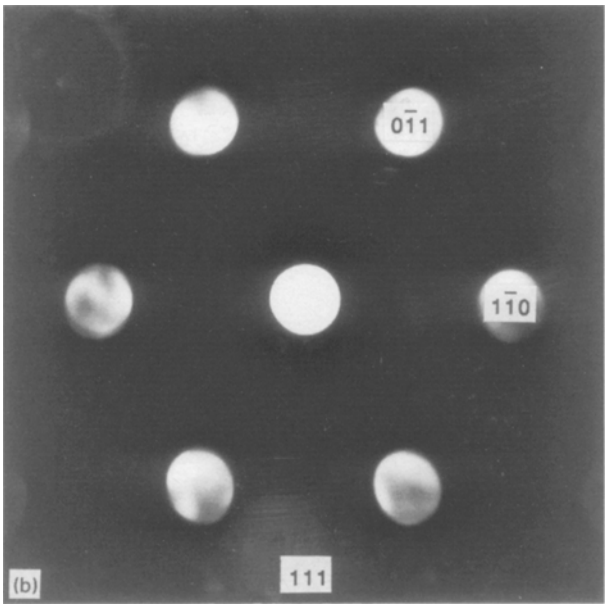

Figure 2 (a) EDXS spectrum and (b) CBED pattern obtained from the SiC layer in the fibre. The SiC layer contained a small amount of Al to form SiC–Al solid solutions.

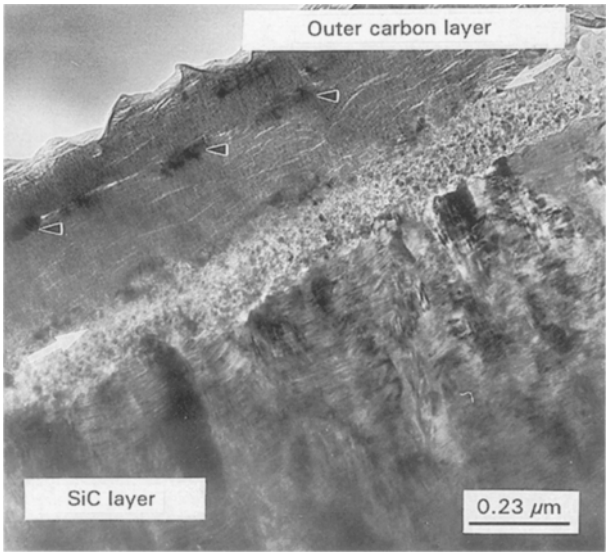

Figure 3 Bright field image of small equiaxed SiC grains on the outside of the columnar SiC grains before the growing of outer carbon layer.

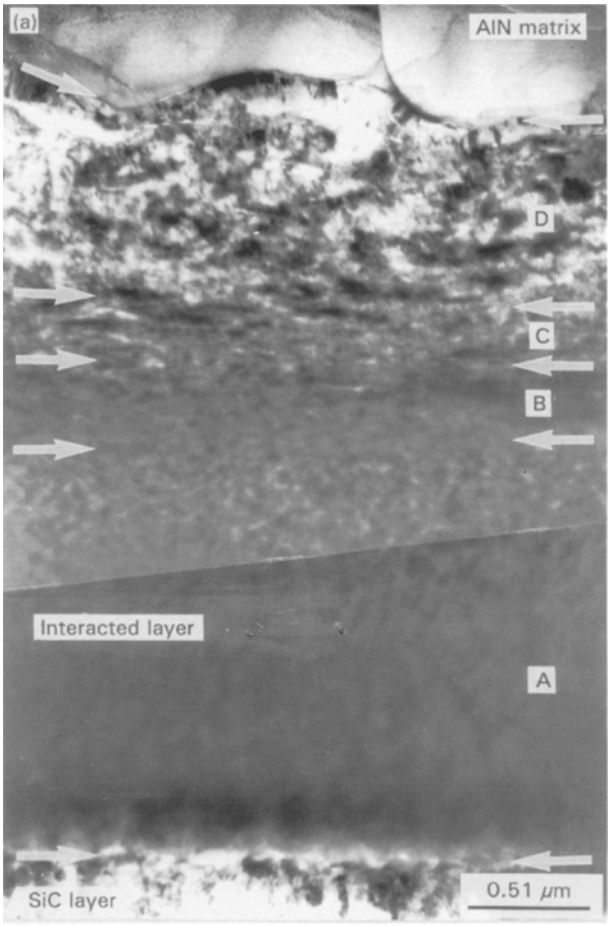

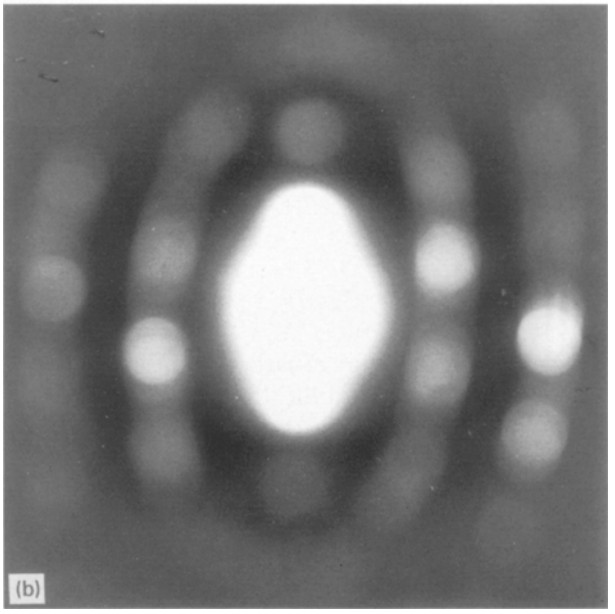

Figure 4 (a) Bright field image of the reacted region of the outermost carbon layer in the fibre and the matrix during fabrication. (b) CBED pattern and (c) EDXS spectrum obtained from the bright area at the reacted layer D shown in (a). (d) SAD pattern and (e) EDXS spectrum obtained from the dark area at the reacted layer D shown in (a).

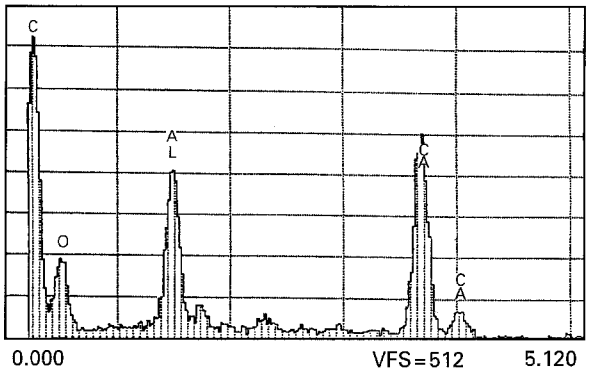

(c)

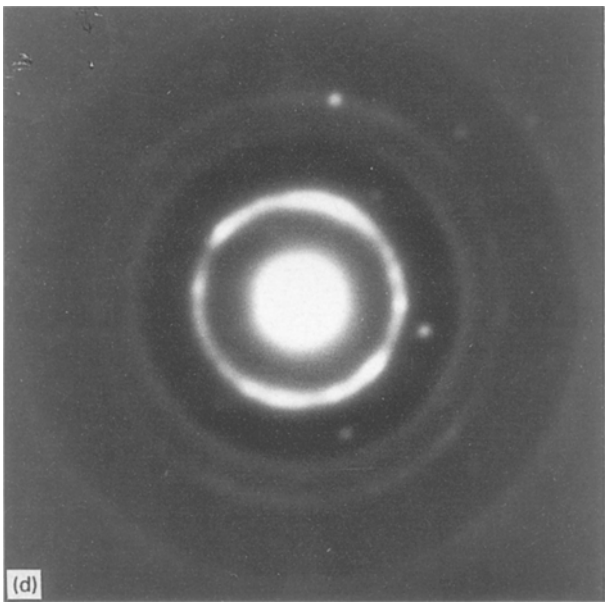

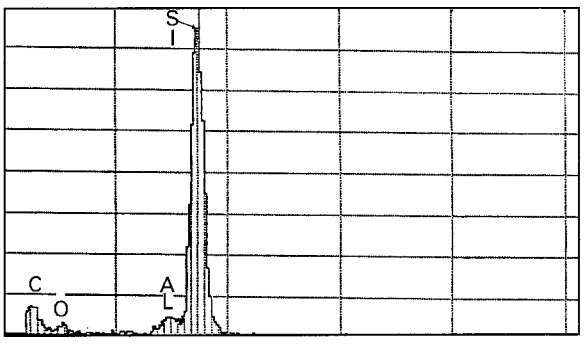

(e)

Figure 4 (continued)

equivalent to a structure of carbon in the outer carbon layer of the unprocessed SiC (SCS-6^{TM}) fibre. A SAD pattern and EDXS spectrum obtained from the Si–Al–C–O phase in the reacted layer D are shown in Fig. 4(d) and (e), respectively. The Si–Al–C–O phase was formed by the reaction of SiC particles in the outermost carbon layer, and Al and O in the matrix, during fabrication. The measured thicknesses of the unreacted sublayers A, B, and C and the reacted layer D shown in Fig. 4(a) are 1.6, 0.3, 0.3 and 1.3 μm, respectively. The outer carbon layer in the unprocessed SiC (SCS-6^{TM}) fibre was found to have a thickness of 3.2 μm and to consist of three sublayers whose thicknesses are 1.6, 0.3 and 1.3 μm, respectively, from the interface between the SiC layer and outer carbon layer towards the matrix radially. Thus, the thicknesses of the outermost carbon layer and AlN matrix interacted during fabrication are 1.0 and 0.3 μm, respectively.

3.2. Room temperature mechanical properties of SiC fibre/AlN composite

The room temperature mechanical properties of monolithic AlN and SiC fibre/AlN composite are shown in Fig. 5. As expected, monolithic AlN shows a linear elastic loading up to a brittle fracture, which is a typical mode of ceramics. The fracture strength and strain to failure of monolithic AlN are 376 MPa and 0.46%, respectively. In contrast, the SiC fibre/AlN composite shows complicated load–deflection behaviours. The composite shows an initial elastic motion before matrix cracking and then a sudden drop in stress at the point of first-matrix cracking. Beyond this point, there is a non-linear loading with increasing deflection, because multiple matrix cracking occurs with possible crack deflections at the matrix/fibre interface. A maximum in load-carrying capacity is expressed as the fracture strength of the composite. Subsequently, stress decreases gradually with increasing strain as intact SiC fibres begin to break and pull

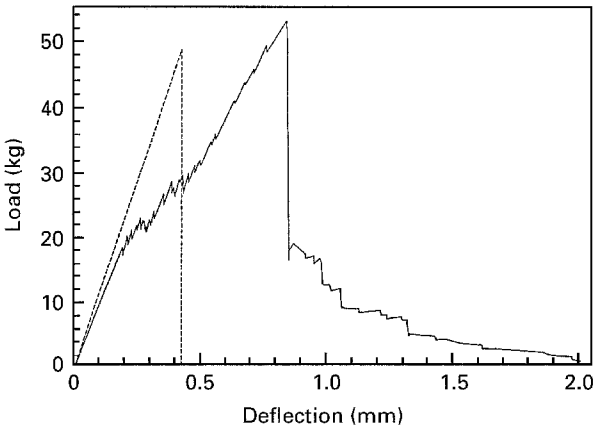

Figure 5 Room-temperature mechanical properties of (– – –) monolithic AlN and (—) SiC fibre/AlN composite.

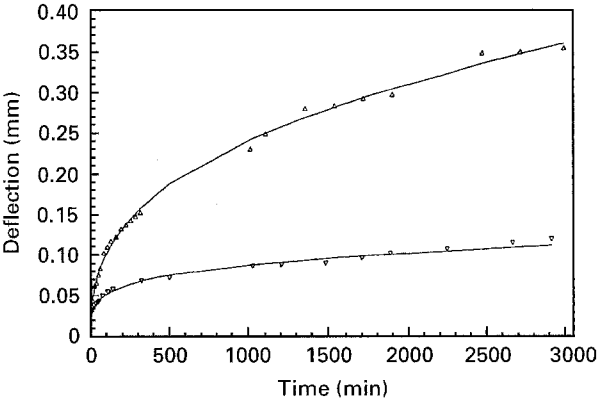

Figure 6 Deflection-time behaviour of (▽) monolithic AlN and (△) SiC fibre/AlN composite measured at 1100 °C and a bending stress of 46.3 MPa for 48 h under oxidizing atmosphere.

out from the matrix. The fracture strength and strain to failure of the composite are 440 MPa and 0.88%, respectively. The SiC fibre provided enhanced room temperature mechanical properties.

3.3. High-temperature creep properties of SiC fibre/AlN composite

Fig. 6 shows a deflection-time behaviour of monolithic AlN and SiC fibre/AlN composite measured at 1100 °C and a bending stress of 46.3 MPa for 48 h under oxidizing condition. This figure exhibits that deflection of the composite is much higher than that of monolithic AlN.

The SEM micrographs of the crept composite showed that most of the cracks were initiated at the reacted regions of the matrix and fibre, and then propagated into the matrix grain boundary (Fig. 7). Detailed microstructure of the crept composite was investigated by analytical TEM, in order to correlate the microstructural features to the high-temperature creep behaviours. There were remarkable differences in the microstructure of the matrix and matrix/fibre interface in the as-fabricated and crept composites. In addition to the $Ca_{12}Al_{14}O_{33}$ formed at the matrix grain boundary during fabrication, pores, cracks, and α-Al_2O_3 were formed at and around matrix grain boundary by the penetration of oxygen during creep test. The cracks were generally associated with the pores and propagated along the matrix grain boundaries. Fig. 8(a) shows a bright field image of the matrix without a crack in the crept composite. The matrix contains $Ca_{12}Al_{14}O_{33}$ (dark area) and α-Al_2O_3 (bright area) phases at the grain boundaries. A CBED pattern obtained from the α-Al_2O_3 is shown in Fig. 8(b).

Fig. 9(a) shows a bright field image of the reacted region of the outer carbon layer in the fibre and the matrix during creep test. The reacted layer consists of two sublayers, which are indicated by A and B in Fig. 9(a). A SAD pattern and EDXS spectrum from the sublayer A are shown in Fig. 9(b) and (c), respectively. The sublayer A was identified as amorphous SiO_2. A SAD pattern and EDXS spectrum from the sublayer B are shown in Fig. 9(d) and (e), respectively. At present, the chemistry and structure of the sublayer B are not determined. The α-Al_2O_3 phase (marked by arrowheads) formed during creep test was present at the reacted layer. The development of pores and α-Al_2O_3 at the matrix grain boundaries and of pores and various oxides (SiO_2, α-Al_2O_3, and Al–Si–C–Ca–O) at the reacted regions of the fibre and matrix caused a bloating of the composite, resulting in a decrease in the high-temperature creep properties. The bloating was also found at the reacted regions of the matrix and fibre by SEM. The volume change resulting from the bloating was estimated as ~3.9%.

Figure 7 SEM micrograph of the crept SiC fibre/AlN composite. Note that crack was initiated at the reacted region of the SiC fibre and matrix.

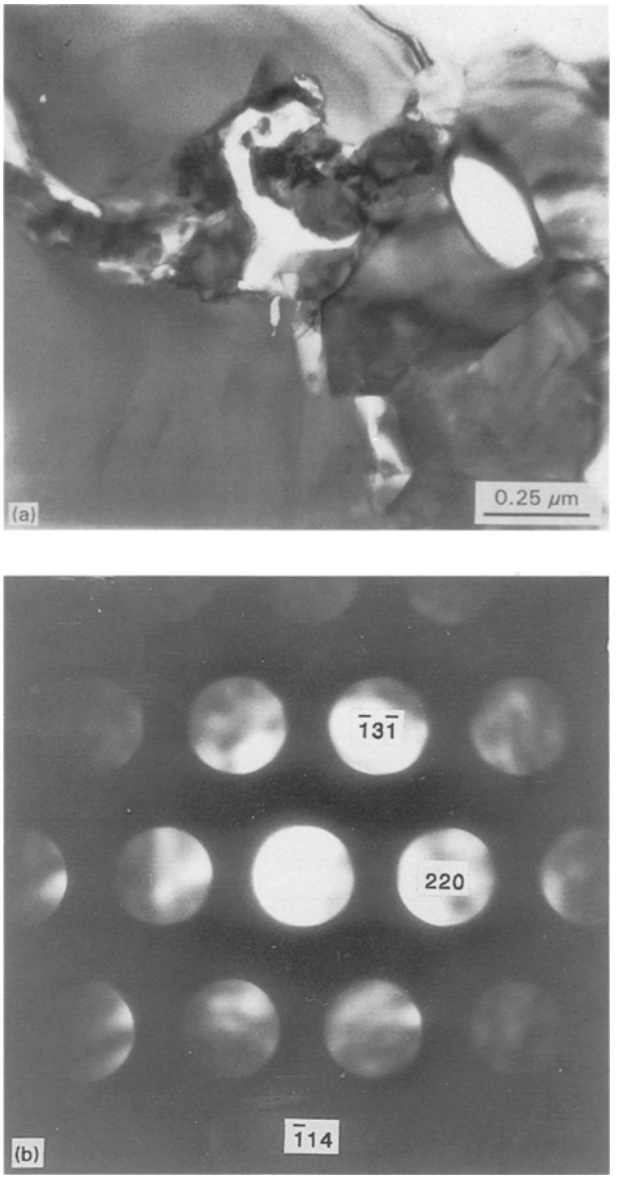

Figure 8 (a) Bright field image of the matrix without a crack in the crept composite. The matrix contains $Ca_{12}Al_{14}O_{33}$ (dark area) and α-Al_2O_3 (bright area) phases at the grain boundaries. (b) CBED pattern obtained from the α-Al_2O_3 at the grain boundaries.

4. Conclusions

Very dense (up to ~ 99% of theoretical density) and fine-grained AlN was fabricated by hot-pressing using $4Ca(OH)_2 \cdot Al_2O_3$ sintering additive at relatively low temperature (1650 °C). It is believed that the sintering

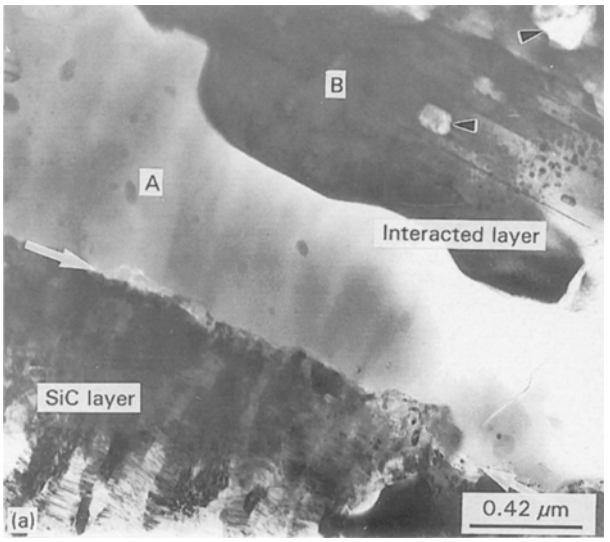

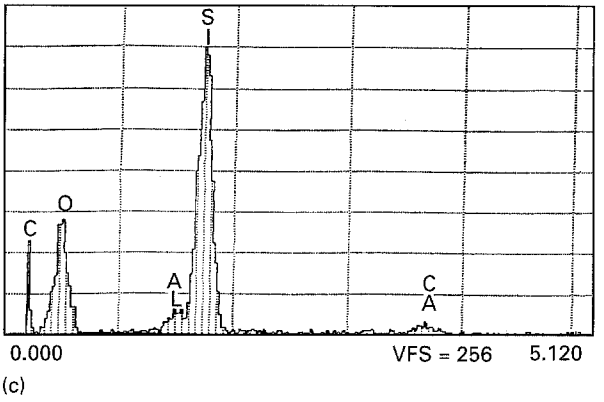

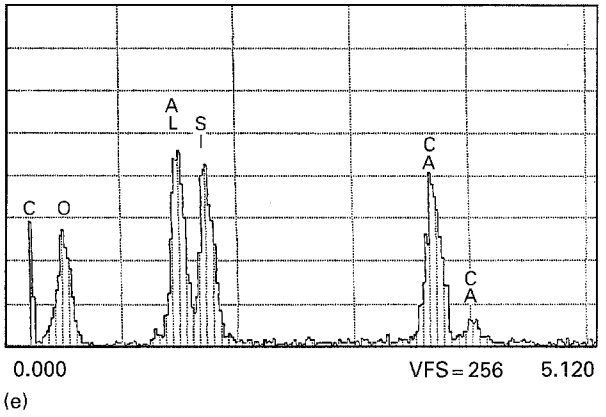

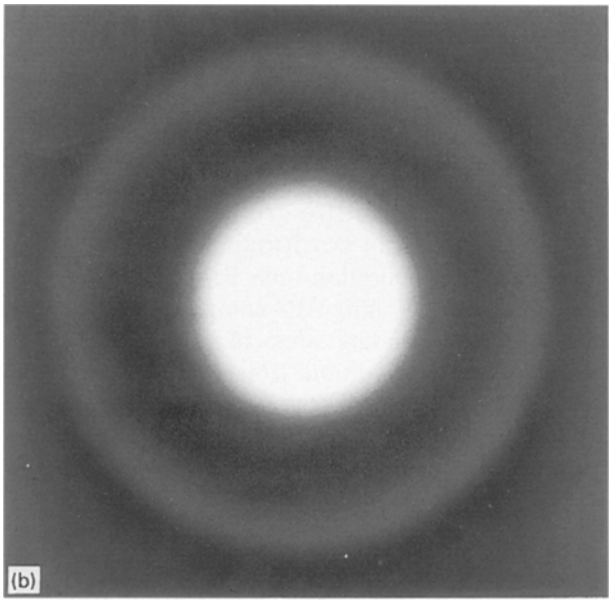

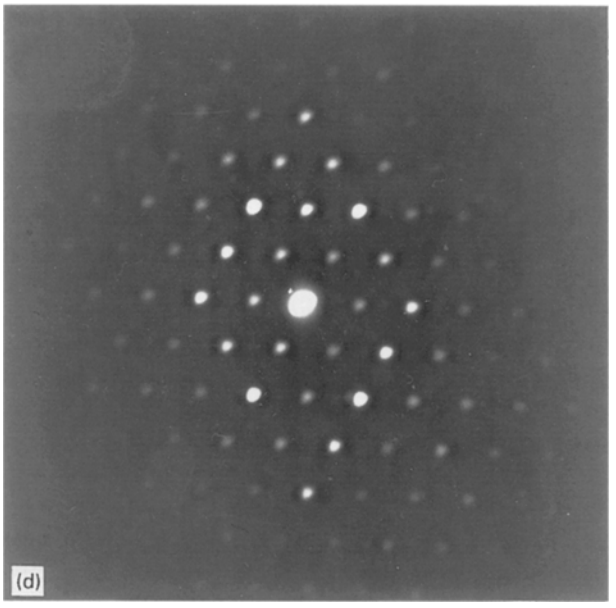

Figure 9 (a) Bright field image of the reacted region of the outer carbon layer in the fibre and the matrix during creep test. (b) SAD pattern and (c) EDXS spectrum obtained from the sublayer A at the reacted region shown in (a). (d) SAD pattern and (e) EDXS spectrum obtained from the sublayer B at the reacted region shown in (a).

additive is very efficient for the densification of AlN. The AlN matrix in the SiC fibre/AlN composite contained rounded grains, $Ca_{12}Al_{14}O_{33}$ liquid phase at grain boundaries, and dislocations within grains. In particular, the SiC fibres maintained their original form and were not degraded during fabrication because of the relatively low sintering temperature. The outermost carbon layer in the fibre reacted with the matrix during fabrication to produce a thin interfacial layer (1.3 μm). The incorporation of SiC fibre into AlN matrix improved significantly the room temperature mechanical properties. This improvement could result from the crack deflections around the SiC fibres. The fracture strength and strain to failure of the composite were 440 MPa and 0.88%, respectively, whereas the fracture strength and strain to failure of monolithic AlN were 376 MPa and 0.46%, respectively.

The microstructure of the matrix and matrix/fibre interface in the composite was changed significantly during creep test. Pores and oxides, such as α-Al_2O_3 and $Ca_{12}Al_{14}O_{33}$, were present at the matrix grain boundaries in the crept composite. Also, pores and oxides, such as SiO_2, α-Al_2O_3, and Al–Si–C–Ca–O, were observed at the reacted regions of the fibre and matrix. The pores and various oxides, which are formed at the matrix grain boundary and matrix/fibre interface during creep test, degraded severely the high-temperature creep properties of the composite.

References

1. Y. KUROKAWA, K. UTSUMI and H. TAKAMIZAWA, *J. Amer. Ceram. Soc.* **71** (1988) 588.

2. Brochure produced by Textron Specialty Materials, Lowell, MA, USA.
3. A. F. VIRKAR, T. B. JACKSON and R. A. CUTLER, *J. Amer. Ceram. Soc.* **72** (1989) 2031.
4. A. KRANZMANN, P. GREIL and G. PETROW, *Sci. Sintering* **20** (1988) 135.
5. ASTM D790, ASTM, Philadelphia, PA, 1993.
6. ASTM C1161, ASTM, Philadelphia, PA, 1993.
7. Y. TAJIMA and W. D. KINGERY, *J. Amer. Ceram. Soc.* **65** (1982) C27.

Received 31 October 1995
and accepted 13 February 1996